JACS
JOURNAL OF THE AMERICAN CHEMICAL SOCIETY
Communication
pubs.acs.org/JACS

Carbon Dioxide Conversion to Methanol over Size-Selected Cu_4 Clusters at Low Pressures

Cong Liu,[†,▽] Bing Yang,[†,▽] Eric Tyo,[†] Soenke Seifert,[‡] Janae DeBartolo,[‡] Bernd von Issendorff,[§] Peter Zapol,*[,†] Stefan Vajda,*[,†,∥,⊥,#] and Larry A. Curtiss*[,†]

[†]Materials Science Division, [‡]X-ray Science Division, and [∥]Nanoscience and Technology Division, Argonne National Laboratory, 9700 S. Cass Ave., Lemont, Illinois 60439, United States

[§]Physikalisches Institut, Universität Freiburg, Stefan-Meier-Straße 21, 79104 Freiburg, Germany

[⊥]Department of Chemical and Environmental Engineering, School of Engineering & Applied Science, Yale University, 9 Hillhouse Avenue, New Haven, Connecticut 06520, United States

[#]Institute for Molecular Engineering, University of Chicago, 5801 South Ellis Avenue, Chicago, Illinois 60637, United States

Supporting Information

ABSTRACT: The activation of CO_2 and its hydrogenation to methanol are of much interest as a way to utilize captured CO_2. Here, we investigate the use of size-selected Cu_4 clusters supported on Al_2O_3 thin films for CO_2 reduction in the presence of hydrogen. The catalytic activity was measured under near-atmospheric reaction conditions with a low CO_2 partial pressure, and the oxidation state of the clusters was investigated by *in situ* grazing incidence X-ray absorption spectroscopy. The results indicate that size-selected Cu_4 clusters are the most active low-pressure catalyst for catalytic CO_2 conversion to CH_3OH. Density functional theory calculations reveal that Cu_4 clusters have a low activation barrier for conversion of CO_2 to CH_3OH. This study suggests that small Cu clusters may be excellent and efficient catalysts for the recycling of released CO_2.

The industrial process of methanol (CH_3OH) synthesis from syngas (CO, CO_2 and H_2) is carried out at high pressures (10 to 100 bar) using a $Cu/ZnO/Al_2O_3$ catalyst.[1] Due to increasing emission of CO_2 from fossil fuel combustion and other anthropogenic activities, this catalytic system has also become the focus of interest for obtaining sustainable CH_3OH by hydrogenation of captured CO_2 ($CO_2 + 3H_2 \rightarrow CH_3OH + H_2O$).[2,3] Efforts have been made to modify and improve the industrial $Cu/ZnO/Al_2O_3$ catalyst.[3−5] Nevertheless, the high pressure required for achieving a quality yield of CH_3OH using these catalysts brings a great challenge for reducing the energy input and cost for this process. Also, effective catalysts are in need for alternative feed streams with lower CO_2 concentrations. Thus, developing an effective low-pressure catalyst for CO_2 reduction to CH_3OH is highly attractive.

Recently, size-selected subnanometer transition metal clusters have received considerable attention in catalysis, because of their unique electronic and catalytic properties, which differ from bulk metal surfaces and larger nanoparticles. Although a number of computational and experimental studies have been focused on catalytic and electrocatalytic CO_2 reduction to fuels on various metal clusters[6−8] and larger nanoparticles,[9−13] there is a paucity of research on CH_3OH synthesis from CO_2 and H_2 on size-selected nonprecious metal clusters. Previously, we have successfully synthesized subnanometer metal clusters with narrow size distributions on thin-film support materials (e.g., Al_2O_3 and Fe_3O_4), and these materials have shown great potential in the catalytic conversion of small molecules.[14−16] Here, we report on Al_2O_3 supported Cu_4 clusters as an effective catalyst for the reduction of CO_2 to CH_3OH at a low CO_2 partial pressure (0.013 atm), with a higher activity than those of recently developed low-pressure catalysts.

Cu_4 clusters were synthesized using a size-selected cluster source,[17] which enables single-size mass selection with atomic precision without fragmentation.[18] The Cu_4 cluster was chosen based on preliminary density functional theory (DFT) calculations indicating they are active for methanol formation. By soft landing, 7 ng of Cu_4^+ clusters were deposited onto a three monolayer amorphous Al_2O_3 thin film prepared by atomic layer deposition (ALD) on top of the native oxide of silicon wafer ($SiO_2/Si(100)$). The detailed description of the preparation method can be found in the previous report.[17] Previous studies have also shown that such a film can keep a variety of clusters from sintering under reaction conditions.[15,16,19] All samples were exposed to air after synthesis, and oxidized copper clusters were identified in the subsequent characterization. The catalytic testing and grazing-incidence X-ray absorption near edge structure (GIXANES) measurements of Al_2O_3 supported Cu_4 clusters were performed in a home-built reaction cell[14,20,21] that allows for X-ray scattering off the sample surface at a grazing incident angle ($\alpha_c = 0.18°$) (details see Supporting Information, SI). All measurements were carried out under *in situ* conditions with 20 sccm flow of 1% CO_2 and 3% H_2 gas mixture carried in helium at a total pressure of 1.25 atm.

The characteristic GIXANES features at the Cu K-edge[22] reflect the evolution of the oxidation state of supported Cu_4 clusters under *in situ* reaction conditions, as displayed in Figure S1a. By comparing the absorption edge of the reference spectra (Cu foil and Cu_2O and CuO bulk standards in Figure S1b), a gradual reduction of Cu_4 clusters under reaction conditions

Received: April 13, 2015
Published: June 26, 2015

DOI: 10.1021/jacs.5b03668
J. Am. Chem. Soc. 2015, 137, 8676−8679

(CO_2/H_2 gas feed) can be identified upon heating to 425 °C. To show the trend in the evolution of the average valence state of copper clusters, a quantitative linear combination fit (LCF) is performed using Cu (Cu^0), Cu_2O (Cu^+), and CuO (Cu^{2+}) bulk standards. Figure 1 presents the LCF results as well as the average

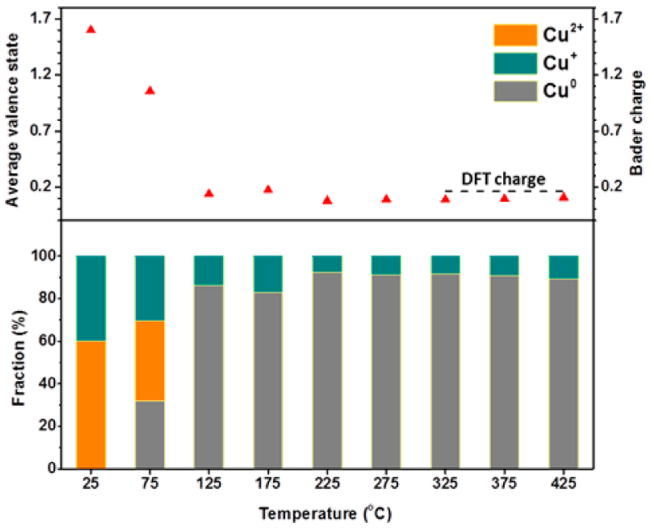

Figure 1. Oxidation state of Al_2O_3 supported Cu_4 clusters at different temperatures under *in situ* catalytic reaction conditions (3% H_2, 1% CO_2 and 96% He, 1.25 atm): (a) Average valence state of Cu_4 clusters. The inserted dashed line indicates the calculated charge from DFT for comparison. (b) LCF results of XANES spectra using bulk Cu foil and Cu_2O and CuO powder as reference materials.

valence state of Cu_4 clusters with increasing reaction temperature. At room temperature, Cu_4 clusters can be described as primarily composed of oxidized Cu^{2+} (~60%) and Cu^+ (~40%), with an average valence state of 1.60. At 75 °C a partial reduction takes place, yielding an average copper valence of 1.05. Starting at 125 °C, the Cu_4 clusters are practically fully reduced as indicated by the ~0.1 average valence state (Figure 1). The observed nonzero value can be ascribed to some charge transfer to a fully reduced (i.e., Cu^0) cluster from either the alumina support or adjacent acidic hydroxyls on the surface.[23,24]

The turnover rate (TOR) of methanol formation from CO_2 hydrogenation over supported Cu_4 clusters is shown in Figure 2. Here, the TOR is defined as the yield of methanol formed per

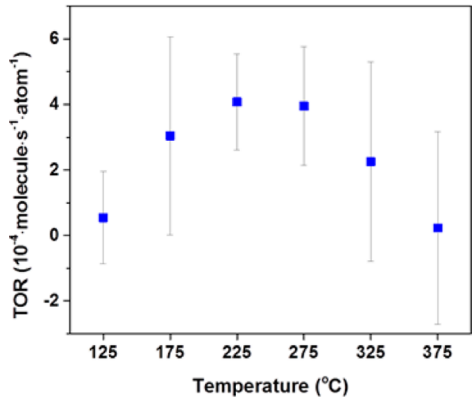

Figure 2. TOR of CO_2 reduction to CH_3OH over Al_2O_3 supported Cu_4 clusters. The data plot is converted from Figure S2b, by averaging 100 data points at each temperature.

copper atom per second. As discussed earlier, under the reaction conditions, the catalyst becomes Cu^0 when 125 °C is reached. This is also the temperature at which CH_3OH starts to be produced, suggesting that the reduction of CO_2 to CH_3OH is mainly catalyzed by the fully reduced state of the Cu_4 clusters. As displayed in Figure 2, the maximal TOR of $\sim 4 \times 10^{-4}$ molecule·s^{-1}·$atom^{-1}$ was obtained at 225 °C, and the rate of methanol production drops above 325 °C, which falls into the thermodynamic control regime.[25] The observed TOR for methanol synthesis is fairly high in comparison to the numbers in the literature.[25,26] Table 1 lists the TOR's of CO_2 reduction to CH_3OH for the present catalyst (Al_2O_3 supported Cu_4 clusters) and recently developed low-pressure catalyst (Ni_5Ga_3/SiO_2) as well as bulk Cu materials ($Cu/ZnO/Al_2O_3$ and polycrystalline Cu foil). It is clear that all the materials reached the maximum activity of CH_3OH in a similar temperature range, 200−240 °C. Compared to Ni_5Ga_3/SiO_2 and $Cu/ZnO/Al_2O_3$ at the ambient pressure, our catalyst demonstrated much higher activity (1 order of magnitude higher) at a slightly higher total pressure (1.25 atm), but with much lower partial pressures (down by up to 2 orders of magnitude) of the reaction gases (H_2 and CO_2), although this activity of the supported Cu_4 clusters is lower than that of the polycrystalline Cu surface under a 6 times higher pressure (Table 1). It clearly shows an outstanding activity of the supported Cu_4 clusters for CO_2 reduction to CH_3OH at a low pressure.

In terms of methane formation ($CO_2 + 4H_2 \rightarrow CH_4 + 2H_2O$), no CH_4 (m/z 15) was obtained as a product below 325 °C, see Figure S2. This indicates that methanation is not favorable in this temperature range. Nevertheless, we obtain an increasing CH_4 signal at 375 °C accompanied by a rise of m/z 18 signal of water, which likely implies the preference of methanation over methanol synthesis at higher temperatures. However, above 375 °C, we also observed the background desorption of hydrocarbon traces (m/z 43 and 56). We note that the fragmentation pattern of these hydrocarbons may also contribute to the CH_4 (m/z 15) signal in the mass spectrometer. Thus, to draw an affirmative conclusion on the high-temperature selectivity of CH_4, further experiments, e.g., with higher sample loading/purified gas feed, are needed, which is beyond the scope of this paper.

Copper may also catalyze a reverse water−gas shift reaction (rWGS, $CO_2 + H_2 \rightarrow CO + H_2O$)[26,27] at high temperatures. A clear assignment of CO (m/z =28) with mass spectrometry is not feasible in our experiments due to its overlap with fragment ions of CO_2 in the feedstock. However, we observe an increasing water signal (m/z 18) above 375 °C when the TOR of methanol synthesis declines (see SI). This is a strong indication of other reaction pathways for CO_2 conversion at elevated temperatures, e.g., rWGS or methanation.

DFT calculations were carried out to help understand the reaction mechanism of the catalytic reduction of CO_2. The Al_2O_3 supported Cu_4 cluster (Cu_4/Al_2O_3) was constructed by binding the Cu_4 cluster onto a hydroxylated amorphous Al_2O_3 surface model obtained from a molecular dynamics (MD) simulation.[28] A GGA_PBE functional[29] with a plane wave basis set was used for geometry optimization and energy calculations. (see SI). The average charge on the supported Cu_4 cluster is found to be +0.16 lel/atom using Bader charge analysis.[30] In the cluster, the two Cu atoms that are bound to the surface oxygens/hydroxyls have slightly positive charges, while the other two Cu atoms carry no charge (see SI). This agrees well with the experimental measurements that the catalyst is mainly fully reduced Cu

DOI: 10.1021/jacs.5b03668
J. Am. Chem. Soc. 2015, 137, 8676−8679

Table 1. Comparison of TOR/TOF of the Present Work and Previous Studies

catalyst	temperature (°C)	total pressure (atm)	partial pressure of H_2 (atm)	partial pressure of CO_2 (atm)	max TOR/TOF of CH_3OH (molecule·s^{-1}·$atom^{-1}$)	ref
Cu_4/Al_2O_3	225	1.25	0.038	0.013	4.0×10^{-4}(TOR)	this work
Ni_5Ga_3/SiO_2	200−220	1	0.75	0.25	6.7×10^{-5} (TOF)[a]	25
$Cu/ZnO/Al_2O_3$	200−220	1	0.75	0.25	6.7×10^{-5} (TOF)[a]	25
polycrystalline Cu foil	237	5	4.6	0.4	1.2×10^{-3} (TOR)	26

[a]These values were converted from the graphs in ref 25.

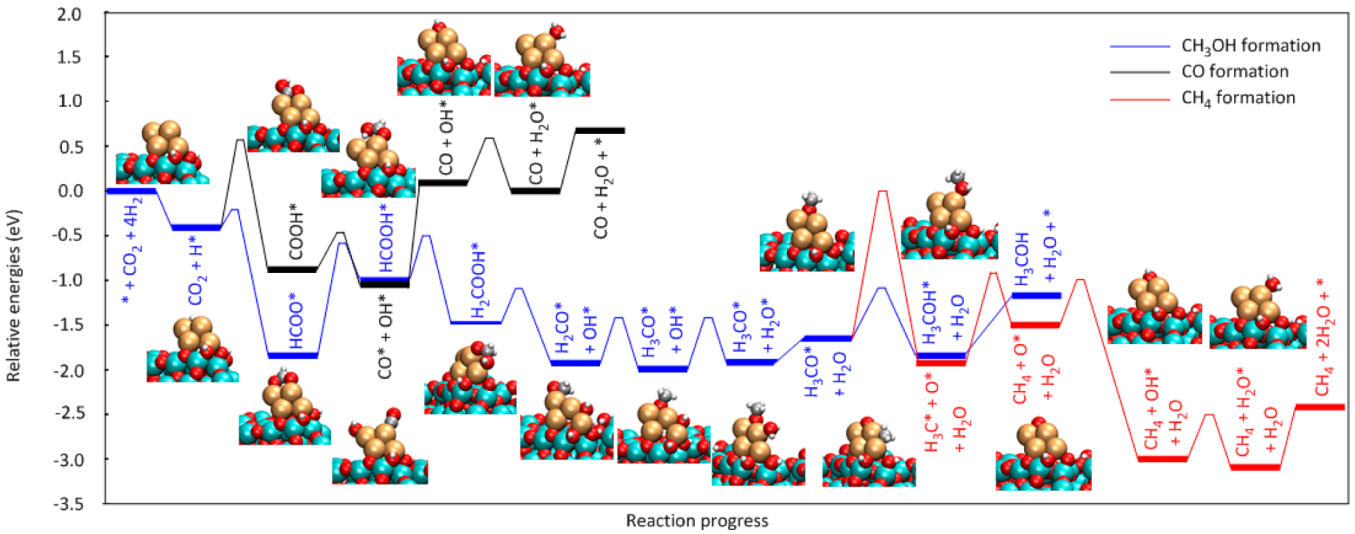

Figure 3. Calculated reaction pathways of CO_2 reduction to CH_3OH, CO and CH_4 on Al_2O_3 supported Cu_4 clusters. The catalyst surface site is labeled as "*". To improve legibility, "H_2" was omitted from the labels after the initial state.

(Figure 1). The slightly positive charges on the bound Cu atoms are due to the partial oxidation of Cu by the bridging O atoms and the hydroxyl groups on the support. The calculated reaction pathways for the CO_2 reduction to CH_3OH, CO and CH_4 on Cu_4 are shown in Figure 3. In general, the calculated reaction mechanism of CH_3OH formation on a supported Cu_4 cluster is similar to that on bulk Cu materials as reported in previous investigations.[3,8,31] The initial step of CH_3OH formation is the formation of the HCOO* species ("*" represents an adsorbed species). The hydrogenation of the HCOO* species produces HCOOH*, which is further hydrogenated to H_2COOH*. Cleavage of the C−OH bond of H_2COOH* leads to its dissociation into H_2CO* and OH*, followed by further hydrogenation of H_2CO* to H_3CO* and OH* to H_2O*. The hydrogenation of H_3CO* generates the final product, CH_3OH. The rate-limiting step of the CH_3OH pathway on Cu_4 is found to be the hydrogenation of the HCOO* species with a predicted barrier of 1.18 eV. This barrier for the Cu_4 cluster is lower than the predicted rate-limiting barriers for the Cu (111) surface (1.60 eV) and the Cu_{29} cluster (1.41 eV), both of which were calculated using a GGA_PW functional by Yang et al.[8] It is also notable that the reaction pathway of the Cu_4 cluster is energetically lower-lying than that of the Cu_{29} cluster, which is lower than that of the Cu(111) surface.[8] This indicates that the Cu_4 cluster could be more active for CH_3OH formation compared to bulk Cu surfaces and larger Cu nanoparticles.

The low reaction barrier for Cu_4 can be explained by the adsorption strength of the adsorbate species to the catalyst. Under-coordinated Cu sites in Cu_4 clusters lead to strong adsorption energies of the adsorbates as found in previous studies of subnanometer clusters,[14] resulting in an energetically lower-lying reaction pathway and a lower barrier. Previous work[3−5] has illustrated that high CO_2 and H_2 pressures increase adsorption energies and make the formation of methanol energetically more favorable. This is why high pressures are needed for CO_2 reduction on Cu surfaces.[3−5] It is further consistent with how the strong adsorption of the adsorbates on the under-coordinated Cu_4 clusters leads to high activity at low CO_2 and H_2 pressures.

For comparison, the reaction pathways for the CO_2 reduction to CO (rWGS) and CH_4 were also investigated (Figure 3). In agreement with a previous DFT study,[32] our calculations showed that the formation of COOH* on Cu_4, which initiates rWGS, has much higher barrier (1.08 eV) than that of HCOO* (0.18 eV), and the rWGS pathway is energetically higher-lying than the CH_3OH pathway. This suggests that the CH_3OH formation is likely to be predominant at lower temperatures for Cu_4. However, at higher temperatures rWGS could become significant due to a bigger reaction rate consistent with the decreasing signal of CH_3OH above 325 °C (Figure 2). CH_4 formation, on the other hand, follows the same path as CH_3OH formation to form the H_3CO* species. Then, the breaking of the C−O bond of H_3CO* leads to H_3C* and O*, after which H_3C* is hydrogenated to CH_4 and O* is finally hydrogenated to H_2O. The rate-limiting step of the CH_4 pathway ($H_3CO^* \rightarrow CH_3^* + O^*$) has a much higher barrier (1.69 eV) than that of the CH_3OH pathway, suggesting that the CH_4 formation would require a much higher reaction temperature than CH_3OH formation. This result supports our experimental observations that CH_3OH was obtained as the main product at a lower temperature range (<375 °C) and explains why Cu clusters favor the CH_3OH formation by the gas-phase hydrogenation of CO_2 rather than the CH_4 formation, even though the net reaction of the latter is thermodynamically more favorable.

DOI: 10.1021/jacs.5b03668
J. Am. Chem. Soc. 2015, 137, 8676−8679

To conclude, to our best knowledge the Al_2O_3 supported size-selected Cu_4 clusters exhibit the highest reported activity to date for CO_2 reduction to CH_3OH at a low CO_2 partial pressure. The unique coordination environment of Cu atoms in size-selected subnanometer clusters results in the active sites that are superior to those of larger Cu particles. These results for size-selected Cu clusters demonstrate their great potential for the development of novel low-pressure catalysts for CH_3OH synthesis from catalytic conversion of CO_2 using alternative feed streams with low CO_2 concentration.

■ ASSOCIATED CONTENT

Supporting Information

The supporting information includes experimental details (methods and reaction conditions), *in-situ* GIXANES measurement, multiple ion detection (MID) analysis of reaction products and computational details (methods and calculated energy data). The Supporting Information is available free of charge on the ACS Publications website at DOI: 10.1021/jacs.5b03668.

■ AUTHOR INFORMATION

Corresponding Authors

*zapol@anl.gov
*vajda@anl.gov
*curtiss@anl.gov

Author Contributions

$^{\nabla}$C.L. and B.Y. contributed equally.

Notes

The authors declare no competing financial interest.

■ ACKNOWLEDGMENTS

This work was supported by the U.S. Department of Energy, Office of Science, BES-Division of Materials Science and Engineering and BES-Scientific User Facilities under Contract DE-AC02-06CH11357. We acknowledge the computing resources operated by the Laboratory Computing Resource Center (ANL) and the ANL Center for Nanoscale Materials. We also thank Dr. Alex Martinson (ANL) for ALD coating. We thank the support of the Director's Postdoctoral Fellowship from ANL to Dr. Cong Liu.

■ REFERENCES

(1) Waugh, K. C. *Catal. Today* **1992**, *15*, 51.
(2) Olah, G. A. *Angew. Chem., Int. Ed.* **2005**, *44*, 2636.
(3) Behrens, M.; Studt, F.; Kasatkin, I.; Kühl, S.; Hävecker, M.; Abild-Pedersen, F.; Zander, S.; Girgsdies, F.; Kurr, P.; Kniep, B.-L.; Tovar, M.; Fischer, R. W.; Nørskov, J. K.; Schlögl, R. *Science* **2012**, *336*, 893.
(4) Yang, Y.; White, M. G.; Liu, P. *J. Phys. Chem. C* **2012**, *116*, 248.
(5) Graciani, J.; Mudiyanselage, K.; Xu, F.; Baber, A. E.; Evans, J.; Senanayake, S. D.; Stacchiola, D. J.; Liu, P.; Hrbek, J.; Sanz, J. F.; Rodriguez, J. A. *Science* **2014**, *345*, 546.
(6) Liu, C.; He, H.; Zapol, P.; Curtiss, L. A. *Phys. Chem. Chem. Phys.* **2014**, *16*, 26584.
(7) Kauffman, D. R.; Alfonso, D.; Matranga, C.; Qian, H.; Jin, R. *J. Am. Chem. Soc.* **2012**, *134*, 10237.
(8) Yang, Y.; Evans, J.; Rodriguez, J. A.; White, M. G.; Liu, P. *Phys. Chem. Chem. Phys.* **2010**, *12*, 9909.
(9) Kwak, J. H.; Kovarik, L.; Szanyi, J. *ACS Catal.* **2013**, *3*, 2449.
(10) Reske, R.; Mistry, H.; Behafarid, F.; Roldan Cuenya, B.; Strasser, P. *J. Am. Chem. Soc.* **2014**, *136*, 6978.
(11) Centi, G.; Perathoner, S.; Winé, G.; Gangeri, M. *Green Chem.* **2007**, *9*, 671.
(12) Gangeri, M.; Perathoner, S.; Caudo, S.; Centi, G.; Amadou, J.; Bégin, D.; Pham-Huu, C.; Ledoux, M. J.; Tessonnier, J. P.; Su, D. S. *Catal. Today* **2009**, *143*, 57.
(13) Rodriguez, J. A.; Evans, J.; Feria, L.; Vidal, A. B.; Liu, P.; Nakamura, K.; Illas, F. *J. Catal.* **2013**, *307*, 162.
(14) Lei, Y.; Mehmood, F.; Lee, S.; Greeley, J.; Lee, B.; Seifert, S.; Winans, R. E.; Elam, J. W.; Meyer, R. J.; Redfern, P. C.; Teschner, D.; Schlogl, R.; Pellin, M. J.; Curtiss, L. A.; Vajda, S. *Science* **2010**, *328*, 224.
(15) Vajda, S.; Pellin, M. J.; Greeley, J. P.; Marshall, C. L.; Curtiss, L. A.; Ballentine, G. A.; Elam, J. W.; Catillon-Mucherie, S.; Redfern, P. C.; Mehmood, F.; Zapol, P. *Nat. Mater.* **2009**, *8*, 213.
(16) Lee, S.; Molina, L. M.; Lopez, M. J.; Alonso, J. A.; Hammer, B.; Lee, B.; Seifert, S.; Winans, R. E.; Elam, J. W.; Pellin, M. J.; Vajda, S. *Angew. Chem., Int. Ed.* **2009**, *48*, 1467.
(17) Yin, C.; Tyo, E.; Kuchta, K.; von Issendorff, B.; Vajda, S. *J. Chem. Phys.* **2014**, *140*, 174201.
(18) Lu, J.; Cheng, L.; Lau, K. C.; Tyo, E.; Luo, X.; Wen, J.; Miller, D.; Assary, R. S.; Wang, H.-H.; Redfern, P.; Wu, H.; Park, J.-B.; Sun, Y.-K.; Vajda, S.; Amine, K.; Curtiss, L. A. *Nat. Commun.* **2014**, *5*, 4895.
(19) Vajda, S.; Lee, S.; Sell, K.; Barke, I.; Kleibert, A.; von Oeynhausen, V.; Meiwes-Broer, K. H.; Rodriguez, A. F.; Elam, J. W.; Pellin, M. M.; Lee, B.; Seifert, S.; Winans, R. E. *J. Chem. Phys.* **2009**, *131*, 121104.
(20) Wyrzgol, S. A.; Schafer, S.; Lee, S.; Lee, B.; Di Vece, M.; Li, X. B.; Seifert, S.; Winans, R. E.; Stutzmann, M.; Lercher, J. A.; Vajda, S. *Phys. Chem. Chem. Phys.* **2010**, *12*, 5585.
(21) Sungsik, L.; Byeongdu, L.; Seifert, S.; Vajda, S.; Winans, R. E. *Nucl. Instrum. Methods Phys. Res., Sect. A* **2011**, *649*, 200.
(22) Stotzel, J.; Lutzenkirchen-Hecht, D.; Frahm, R.; Kimmerle, B.; Baiker, A.; Nachtegaal, M.; Beier, M. J.; Grunwaldt, J. D. Proceedings of the *14th International Conference on X-Ray Absorption Fine Structure (XAFS14)*; Institute of Physics Publishing (IOP): London, 2009; Vol. *190*.
(23) Mason, M. G. *Phys. Rev. B: Condens. Matter Mater. Phys.* **1983**, *27*, 748.
(24) Hellman, A.; Gronbeck, H. *J. Phys. Chem. C* **2009**, *113*, 3674.
(25) Studt, F.; Sharafutdinov, I.; Abild-Pedersen, F.; Elkjær, C. F.; Hummelshøj, J. S.; Dahl, S.; Chorkendorff, I.; Nørskov, J. K. *Nat. Chem.* **2014**, *6*, 320.
(26) Yoshihara, J.; Parker, S. C.; Schafer, A.; Campbell, C. *Catal. Lett.* **1995**, *31*, 313.
(27) Matsubu, J. C.; Yang, V. N.; Christopher, P. *J. Am. Chem. Soc.* **2015**, *137*, 3076.
(28) Adiga, S. P.; Zapol, P.; Curtiss, L. A. *J. Phys. Chem. C* **2007**, *111*, 7422.
(29) Perdew, J. P.; Burke, K.; Ernzerhof, M. *Phys. Rev. Lett.* **1996**, *77*, 3865.
(30) Tang, W. *J. Phys. Cond. Matt.* **2009**, *21*, 084204.
(31) Grabow, L. C.; Mavrikakis, M. *ACS Catal.* **2011**, *1*, 365.
(32) Zhang, R.; Wang, B.; Liu, H.; Ling, L. *J. Phys. Chem. C* **2011**, *115*, 19811.

DOI: 10.1021/jacs.5b03668
J. Am. Chem. Soc. 2015, 137, 8676−8679